

Coverage Analysis of a Thinned LiFi Optical Attocell Network

Atchutananda Surampudi

Department of Engineering Science, University of Oxford, OX1-3PJ, Oxford.
atchutananda.surampudi@wadham.ox.ac.uk

Abstract—This work analyzes coverage in the downlink of a thinned LiFi attocell network of deterministically arranged LEDs. The network is thinned by a Bernoulli probability p over all the LEDs to decide whether each one of them acts as a LiFi source or not. Then we use the series approximation approach used in [1] to obtain closed form expressions for the probability of coverage in such thinned LiFi attocell networks and validate them using numerical simulations.

Index Terms— Attocell dimension, interference, LiFi, light emitting diode, photodiode.

I. INTRODUCTION

Light Fidelity (LiFi) has emerged as a high speed wireless data access solution using visible light [2]. For downlink access, the arrangement of a network of LiFi sources using light emitting diodes (LEDs) is called an attocell network. Such an attocell network is centrally monitored and is generally arranged in a deterministic lattice. In many situations, for example in a large conference room or a library, out of such a deterministic lattice arrangement, all the LEDs providing illumination may not be acting as LiFi data access points. Those LEDs that act as LiFi sources are then randomly located over a thinned version of the original deterministic lattice. Modelling such a random point process of LiFi-LEDs has been an open area of research. The Poisson point process (PPP) that is generally used to model conventional wireless networks, cannot be assumed in this case because it does not appropriately consider into account the minimum separation between the randomly located points over a deterministic lattice. The corresponding analysis of the signal-to-interference-plus-noise-ratio (SINR) and the determination of the probability of coverage at a particular receiver also becomes difficult since the time varying fading over the line-of-sight LiFi channels is considered to be absent.

A. Related works

This problem of modelling such a point process of LiFi-LEDs and the analysis of the corresponding probability of coverage has been cited in [3]–[6]. Almost all of them assume a PPP of LiFi-LEDs and derive tractable expressions to analyze coverage under no-fading conditions. But as mentioned earlier, this assumption does not appropriately take into account the minimum separation between the LEDs over the deterministic lattice. Closed form expressions for co-channel interference and SINR have been derived in [1], but only for the case

when all the LEDs are LiFi sources over the lattice without randomness.

B. Our contributions

This work proposes a novel solution to characterize coverage in a thinned LiFi attocell network. Firstly, every LED in the network is assigned a Bernoulli probability p of acting as a LiFi source. Then the interference is modelled as an infinite summation over a set of weighted Bernoulli random variables that are independent. This large sum is approximated to be converging in distribution to a Gaussian random variable whose mean and variance are exactly calculated. The series approximation approach used in [1] is implemented to provide closed form expressions for the mean and the variance, which eventually are used to calculate an exact expression for the probability of coverage over an attocell.

C. Arrangement of the paper

The paper is arranged as follows. Section II describes the system model. Section III is the main technical part of the paper that derives the expression for the probability of coverage. Validations using numerical simulations are presented in Section IV. The paper concludes with Section V.

II. SYSTEM MODEL

A. The attocell network

Consider the infinite¹ two dimensional arrangement of LEDs in Fig.1, all of them fixed at a height h , separated symmetrically by a distance a , and emitting light at a uniform average optical power P_o . Also, the LEDs have a Lambertian emission order $m = -\frac{\ln(2)}{\ln(\cos(\theta_h))}$, where θ_h is the half-power-semi-angle (HPSA) of any given LED. The photodiode (PD) of an area of cross section A_{pd} , responsivity R_{pd} and field-of-view of $\frac{\pi}{2}$ radians is assumed to have its surface always parallel to the ground, i.e., without any orientation towards any LED, and is assumed to be located at $z = \sqrt{z_x^2 + z_y^2}$ from the origin $(0, 0, 0)$. Importantly, the nearest LED at $(0, 0, h)$ is assumed to emit data and the PD is tagged to this LED for LiFi access. For every i^{th} LED, a random variable α_i is assigned that decides whether the LED acts as a LiFi source

¹An infinite network is considered in this work so as to model an ideal environment where the receiver receives interference from all directions and is located in the centre of the network. This assumption is practically equivalent to a large open room.

with probability p , or not with probability $1 - p$. For brevity, α_i is clearly defined as follows.

$$\alpha_i \stackrel{d}{\sim} \begin{cases} p; & \alpha_i = 1, \\ 1 - p; & \alpha_i = 0. \end{cases}$$

This work neglects any non-linearities of the LED while intensity modulation. For the mathematical analysis, let all the LEDs belong to an infinite set \mathbb{S} . Let the modulation bandwidth of the system be W and the noise power spectral density at the PD be N_o . Also, since the LEDs are assumed to be installed in a large open room, the multi-path and non-line-of-sight components received at the PD are considered relatively insignificant in power [7]–[9].

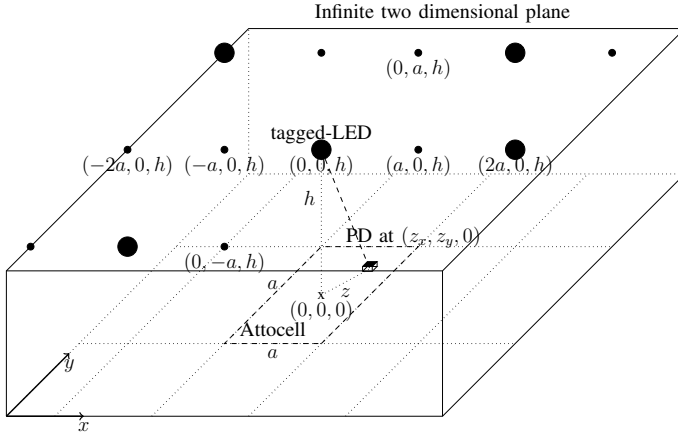


Figure 1. This figure, adapted from [1], shows the infinite two dimensional LED network. There are infinite number of LEDs (circular dots) arranged symmetrically at regular intervals of a all over the plane as a uniform square grid and installed at a height h . The rectangular dotted regions on ground depict the attocells corresponding to each LED above. Those LEDs which provide LiFi data access are depicted as relatively larger circles, while those which are idle are depicted as smaller ones. The user PD (small cuboid) at $(z_x, z_y, 0)$ is assumed to have LiFi access from the tagged-LED at $(0, 0, h)$ and the corresponding attocell is highlighted as dash-dot.

B. The signal-to-interference-plus-noise ratio

Since all the LEDs saving the tagged LED are probably not LiFi enabled sources, the PD receives both unmodulated and modulated interference from the network. By assuming the value of $\alpha_i = 0$ for the unmodulated sources, this work evidently oversees the unmodulated power received at the PD by assuming the fact that this unmodulated interference can be overcome by applying a suitable bias at the receiver or an equivalent high pass filter. Regardless of whether LiFi enabled or not, the optical intensities $s_i(t)$ from every i^{th} LED experience a channel gain $G_i(z)$ given as [1]

$$G_i(z) = K(D_i^2 + h^2)^{\frac{-(m+3)}{2}},$$

where D_i represents the horizontal distance between the PD and the i^{th} LED, and $K = \frac{(m+1)A_{pd}h^{m+1}}{2\pi}$. If $i = 0$ represents the tagged LiFi enabled LED at $(0, 0, h)$, then $D_0 = z = \sqrt{z_x^2 + z_y^2}$. All other LEDs ($i \in \mathbb{S} \setminus 0$) now become co-channel

interferers. The total received current $I(z, t)$ at the PD located at z and during the time slot t is given as

$$I(z, t) = s_0(t)G_0(z)R_{pd} + \mathcal{I}_\infty(z, t) + n(t),$$

where $n(t)$ is the additive white Gaussian noise process with power spectral density N_o , and a variance of $\sigma^2 = N_o W$. Now, we can express the interference $\mathcal{I}_\infty(z, t)$ as

$$\mathcal{I}_\infty(z, t) = \sum_{i \in \mathbb{S} \setminus 0} \alpha_i s_i(t) G_i(z) R_{pd}.$$

So, after performing the time average over the received current, the electrical signal-to-interference-plus-noise ratio $\gamma(z)$ at the PD can be expressed as

$$\gamma(z) = \frac{P_o^2 G_0^2(z) R_{pd}^2}{\sum_{i \in \mathbb{S} \setminus 0} \alpha_i P_o^2 G_i^2(z) R_{pd}^2 + \sigma^2}. \quad (1)$$

The main results for the probability of coverage are presented in the following section.

III. THE PROBABILITY OF COVERAGE

The probability of coverage $P_c(z, \theta)$, against a threshold θ , can be expressed as a spatial average over the attocell dimensions as

$$P_c = \frac{1}{a^2} \int_{-\frac{a}{2}}^{\frac{a}{2}} \int_{-\frac{a}{2}}^{\frac{a}{2}} P_c(z, \theta) dz_x dz_y,$$

where,

$$P_c(z, \theta) = \mathbb{P}[\gamma(z) > \theta | z],$$

$$\begin{aligned} &\stackrel{(a)}{=} \mathbb{P} \left[\sum_{i \in \mathbb{S} \setminus 0} \alpha_i P_o^2 G_i^2(z) R_{pd}^2 < \frac{P_o^2 G_0^2(z) R_{pd}^2}{\theta} - \sigma^2 \middle| z \right], \\ &= \mathbb{P} \left[\sum_{i \in \mathbb{S} \setminus 0} \alpha_i (D_i^2 + h^2)^{-\beta} < \eta \middle| z \right], \\ &= \mathbb{P}[C < \eta | z], \end{aligned} \quad (2)$$

where (a) follows from rearranging (1); $\beta = m + 3$, and $\eta = \frac{G_0^2(z)}{K^2 \theta} - \frac{\sigma^2}{K^2 P_o^2 R_{pd}^2}$; and $C = \sum_{i \in \mathbb{S} \setminus 0} \alpha_i (D_i^2 + h^2)^{-\beta}$ represents the infinite summation over a set of weighted ($w_i = (D_i^2 + h^2)^{-\beta}$) independent and identical (iid) random variables, each of which is distributed as

$$\alpha_i w_i \stackrel{d}{\sim} \begin{cases} p & ; \alpha_i w_i = (D_i^2 + h^2)^{-\beta}, \\ 1 - p; & \alpha_i w_i = 0, \end{cases}$$

with the mean $\mu_i = \mathbb{E}[\alpha_i w_i] = p(D_i^2 + h^2)^{-\beta}$, and variance $\sigma_{i_i}^2 = \text{Var}[\alpha_i w_i] = p(1 - p)(D_i^2 + h^2)^{-2\beta}$. Correspondingly, the mean of C can be expressed as

$$\mu = \mathbb{E}[C] = \sum_{i \in \mathbb{S} \setminus 0} p(D_i^2 + h^2)^{-\beta},$$

and the variance of C can be expressed as

$$\sigma_1^2 = \text{var}[C] = \sum_{i \in \mathbb{S} \setminus 0} p(1 - p)(D_i^2 + h^2)^{-2\beta}.$$

Now, since the summation is over a large number of weighted iid random variables, C is approximated to converge in distribution to a Gaussian with the mean μ and variance σ_1^2 . This approximation is numerically validated with analytical simulations in section IV. As a matter of fact, $D_i^2 = (ua + z_x)^2 + (va + z_y)^2$, represents the horizontal distance of the PD from every other i^{th} LED located at (ua, va, h) . So, the mean and variance can be expanded as $\mu = pS_m$, and $\sigma_1^2 = p(1-p)S_v$, with

$$S_m = \sum_{u=-\infty}^{+\infty} \sum_{v=-\infty \setminus (0,0)}^{+\infty} ((ua + z_x)^2 + (va + z_y)^2 + h^2)^{-\beta},$$

$$S_v = \sum_{u=-\infty}^{+\infty} \sum_{v=-\infty \setminus (0,0)}^{+\infty} ((ua + z_x)^2 + (va + z_y)^2 + h^2)^{-2\beta}.$$

From [1], for a given height to inter-LED separation ratio h/a , we can write a closed form expression for S_m and S_v as follows.

$$S_m \approx S'_m = \frac{h^{2-2\beta}\pi}{a^2(\beta-1)} - \frac{1}{(z^2 + h^2)^\beta} + \sum_{(w,f) \in \mathbb{A}} g_m(w, f), \quad (3)$$

$$S_v \approx S'_v = \frac{h^{2-4\beta}\pi}{a^2(2\beta-1)} - \frac{1}{(z^2 + h^2)^{2\beta}} + \sum_{(w,f) \in \mathbb{A}} g_v(w, f), \quad (4)$$

where $g_m(w, f) =$

$$\frac{\mathbb{K}_{\beta-1} \left(\frac{2\pi h \sqrt{f^2 + w^2}}{a} \right) \cos \left(\frac{2\pi w z_x}{a} \right) \cos \left(\frac{2\pi f z_y}{a} \right)}{\left(\frac{h}{2\pi \sqrt{f^2 + w^2}} \right)^{\beta-1} 2^{\beta-4} a^{\beta+1} \frac{\Gamma(\beta)}{\pi}},$$

$g_v(w, f) =$

$$\frac{\mathbb{K}_{2\beta-1} \left(\frac{2\pi h \sqrt{f^2 + w^2}}{a} \right) \cos \left(\frac{2\pi w z_x}{a} \right) \cos \left(\frac{2\pi f z_y}{a} \right)}{\left(\frac{h}{2\pi \sqrt{f^2 + w^2}} \right)^{2\beta-1} 2^{2\beta-4} a^{2\beta+1} \frac{\Gamma(2\beta)}{\pi}},$$

and the set $\mathbb{A} \triangleq (\mathbb{Z}^2 \cap ([0, j] \times [0, l])) \setminus (0, 0)$ over the set of integers \mathbb{Z}^2 . For most of the practical use-cases, it is sufficient to choose only the terms corresponding to $j = l = 1$, i.e., $(w = 0, f = 1)$, $(w = 1, f = 0)$ and $(w = 1, f = 1)$.

Hence, the P_c can now be extended from (2) as

$$\begin{aligned} P_c &= \int_{-\frac{\pi}{2}}^{\frac{\pi}{2}} \int_{-\frac{\pi}{2}}^{\frac{\pi}{2}} \left[\int_0^\eta \frac{1/a^2}{\sqrt{2\pi}\sigma_1} \exp \left(\frac{-(x-\mu)^2}{2\sigma_1^2} \right) dx \right] dz_x dz_y, \\ &= \int_{-\frac{\pi}{2}}^{\frac{\pi}{2}} \int_{-\frac{\pi}{2}}^{\frac{\pi}{2}} \left(\frac{\text{Erf} \left(\frac{\eta-\mu}{\sqrt{2}\sigma_1} \right) + \text{Erf} \left(\frac{\mu}{\sqrt{2}\sigma_1} \right)}{2a^2} \right) dz_x dz_y, \\ &\stackrel{(a)}{\approx} \int_{-\frac{\pi}{2}}^{\frac{\pi}{2}} \int_{-\frac{\pi}{2}}^{\frac{\pi}{2}} \frac{1}{2a^2} \left(\text{Erf} \left(\frac{\eta - pS'_m}{\sqrt{2}p(1-p)S'_v} \right) \right. \\ &\quad \left. + \text{Erf} \left(\frac{S'_m}{\sqrt{2}(1-p)S'_v} \right) \right) dz_x dz_y, \end{aligned} \quad (5)$$

Table I
PARAMETERS CONSIDERED FOR NUMERICAL SIMULATIONS

Parameter	Symbol	Value	Unit
Temperature of Operation	T	300	K
Noise power spectral density at Photodiode	N_o	4.14×10^{-21}	$\text{A}^2 \text{Hz}^{-1}$
Modulation bandwidth of LED	W	40×10^6	Hz
Area of Photodiode	A_{pd}	10^{-4}	m^2
Responsivity of PD	R_{pd}	0.1	AW^{-1}
Average optical power	P_o	1	W
Half power semi angle of all LEDs	θ_h	$\pi/3$	radians

where $\text{Erf}(x) = \int_0^x \frac{2e^{-t^2}}{\sqrt{\pi}} dt$ is the standard Gaussian error function and (a) follows from the approximation in (3) and (4).

IV. SIMULATION RESULTS

The P_c is validated using both numerical and analytical simulations at various values of $h/a \in \{3, 4, 5, 6\}$, and at different modulation probabilities $p \in \{0.3, 0.5, 0.8\}$ respectively in Fig.3, 2 and 4. Other optical parameters are shown in Table I.

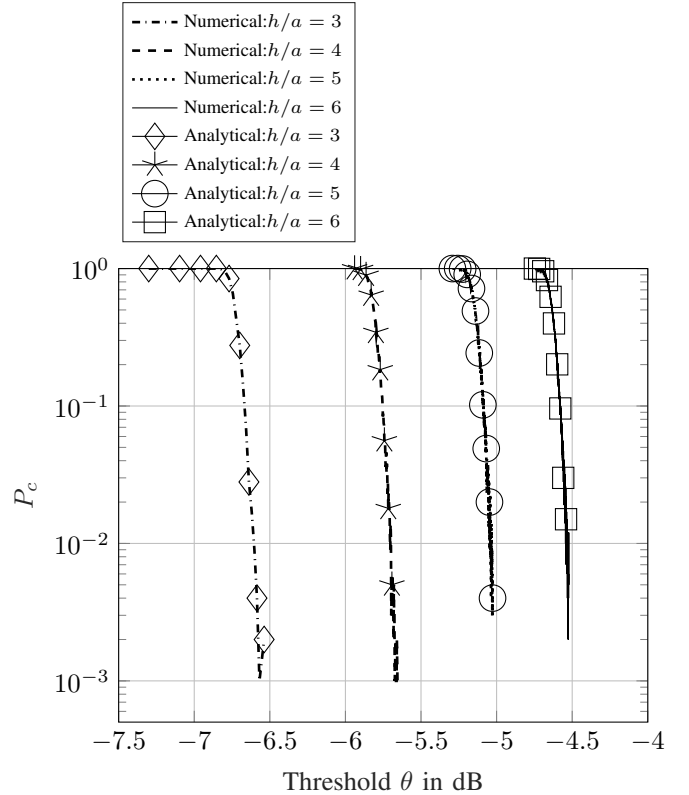


Figure 2. At $p = 0.5$, the variation of probability of coverage P_c is plotted against the threshold θ , for different values of the ratio h/a of LED installation. The ratio h/a is realized by assuming $a = 0.5\text{m}$ and $h \in \{1.5, 2.0, 2.5, 3.0\}\text{m}$.

In Fig.2 for $p = 0.5$, the analytical simulations for the probability of coverage show that the P_c over the central

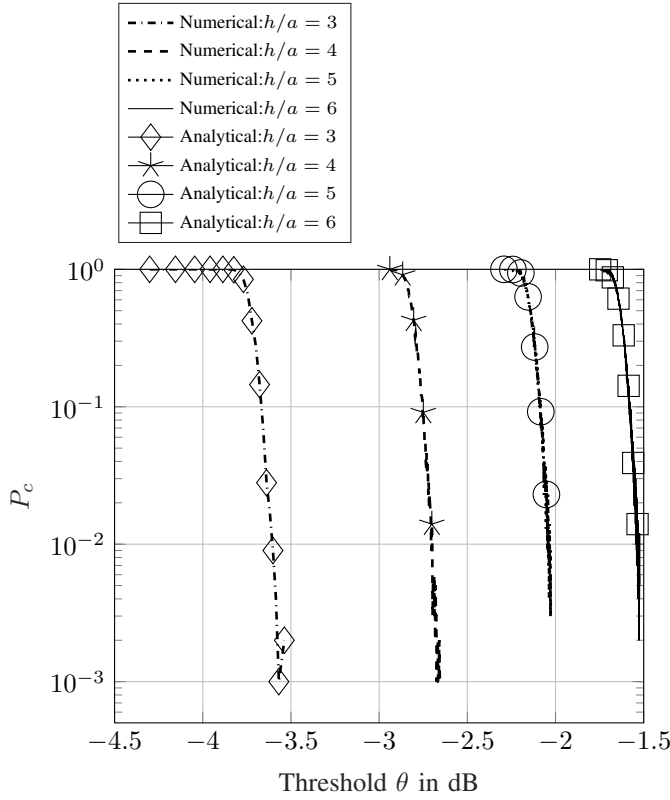


Figure 3. At $p = 0.3$, the variation of probability of coverage P_c is plotted against the threshold θ , for different values of the ratio h/a of LED installation. The ratio h/a is realized by assuming $a = 0.5\text{m}$ and $h \in \{1.5, 2.0, 2.5, 3.0\}\text{m}$.

attocell drops steadily with increase in the SINR threshold θ . But when the ratio h/a increases, this drop in P_c occurs at higher values of θ . For instance at $h/a = 3$, $P_c = 0.6$ is achieved when $\theta = -6.55\text{dB}$; and when h/a is increased to 4, $P_c = 1$ which later drops with an increase in θ beyond -6dB . This also means that for a fixed inter-LED spacing a , more is the height h of LED installation, a better coverage probability occurs even for lower values of the SINR at the PD. Parallely, these analytical results have been validated with appropriate numerical simulations which are tight and are drawn neither with any Gaussian approximation nor the series approximation from [1] for S_m and S_v .

A similar trend can be observed in Fig.3 for $p = 0.3$, and in Fig. 4 for $p = 0.8$ where P_c drops steadily with increase in θ . All the same, this range of θ shifts to a lower threshold band as the modulation probability p increases. This is true because, as p the probability that an LED will be a LiFi source increases, the attocell network will have more LiFi sources. This implies more co-channel interference and as a result lesser probability of coverage P_c .

V. CONCLUSION

This work derived an exact expression for probability of coverage in a LiFi attocell network that is essentially thinned out of a deterministic one. Validations with numerical simu-

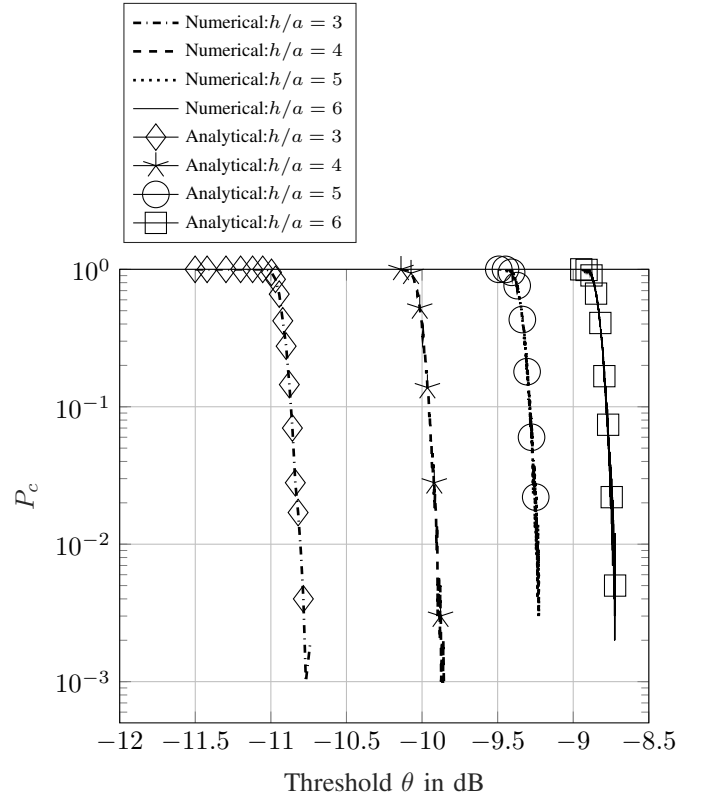


Figure 4. At $p = 0.8$, the variation of probability of coverage P_c is plotted against the threshold θ , for different values of the ratio h/a of LED installation. The ratio h/a is realized by assuming $a = 0.5\text{m}$ and $h \in \{1.5, 2.0, 2.5, 3.0\}\text{m}$.

lations are provided. Analysis of joint transmission schemes shall form a part of the future work.

REFERENCES

- [1] A. Surampudi and R. K. Ganti, "Interference Characterization in Downlink Li-Fi Optical Attocell Networks," *Journal of Lightwave Technology*, vol. 36, no. 16, pp. 3211–3228, 2018.
- [2] Haas, Harald, "LiFi: Conceptions, misconceptions and opportunities," in *Photonics Conference (IPC), 2016 IEEE*. IEEE, 2016, pp. 680–681.
- [3] L. Yin and H. Haas, "Coverage Analysis of Multiuser Visible Light Communication Networks," *IEEE Transactions on Wireless Communications*, vol. 17, no. 3, pp. 1630–1643, 2018.
- [4] C. Chen, D. A. Basnayaka, and H. Haas, "Downlink Performance of Optical Attocell Networks," *Journal of Lightwave Technology*, vol. 34, no. 1, pp. 137–156, 2016.
- [5] L. Yin and H. Haas, "A Tractable Approach to Joint Transmission in Multiuser Visible Light Communication Networks," *IEEE Transactions on Mobile Computing*, p. Early access.
- [6] C. Chen and H. Haas, "Performance Evaluation of Downlink Cooperative Multipoint Joint Transmission in LiFi Systems," in *Globecom Workshops (GC Wkshps), 2017 IEEE*. IEEE, 2017, pp. 1–6.
- [7] T. Komine and M. Nakagawa, "Fundamental Analysis for Visible-Light Communication System Using LED Lights," *IEEE Transactions on Consumer Electronics*, vol. 50, no. 1, pp. 100–107, 2004.
- [8] J. Grubor, S. Randel, K.-D. Langer, and J. W. Walewski, "Broadband Information Broadcasting Using LED-Based Interior Lighting," *Journal of Lightwave Technology*, vol. 26, no. 24, pp. 3883–3892, 2008.
- [9] L. Zeng, D. C. O'Brien, H. Le Minh, G. E. Faulkner, K. Lee, D. Jung, Y. Oh, and E. T. Won, "High Data Rate Multiple Input Multiple Output (MIMO) Optical Wireless Communications Using White LED Lighting," *IEEE Journal on Selected Areas in Communications*, vol. 27, no. 9, 2009.